

The phase of the $\sigma \rightarrow \pi\pi$ amplitude in $J/\Psi \rightarrow \omega\pi^+\pi^-$

D.V. Bugg,
Queen Mary, University of London, London E1 4NS, UK

Abstract

The phase variation of the $\sigma \rightarrow \pi\pi$ amplitude is accurately determined as a function of mass from BES II data for $J/\Psi \rightarrow \omega\pi^+\pi^-$. The determination arises from interference with the strong $b_1(1235)\pi$ amplitude. The observed phase variation agrees within errors with that in $\pi\pi$ elastic scattering.

PACS Categories: 11.80.Et, 13.20.Fe, 13.20.He, 14.40.Lb

The σ pole appears as a conspicuous $\pi^+\pi^-$ peak in BES II data for $J/\Psi \rightarrow \omega\pi^+\pi^-$ [1]. This peak is absent from data on $\pi\pi$ S-wave elastic scattering. The connection between these two processes is a question which is explored here.

For both processes, the partial wave amplitude $f(s)$ may be written

$$f(s) = N(s)/D(s), \quad (1)$$

where $N(s)$ has only left-hand cuts and $D(s)$ has only right-hand cuts. The N function can be different for the two processes. We pursue the hypothesis that $N(s)$ for $\pi\pi$ elastic scattering contains an Adler zero, which is absent from the production process. The phase variation above the $\pi\pi$ threshold arises from the right-hand cut. The D function should be the same for all processes if only a single resonance contributes. The question is whether BES data and $\pi\pi$ elastic scattering data are consistent with this hypothesis.

The Dalitz plot for $J/\Psi \rightarrow \omega\pi^+\pi^-$ is shown in Fig. 1. The σ pole appears as a diagonal band at the upper right-hand edge of this plot. There are also strong vertical and horizontal bands due to $b_1^\pm(1235) \rightarrow \omega\pi^\pm$. These two bands account for 41% of the data; the σ pole accounts for 19% and $f_2(1270)$ for most of the remaining intensity. There is strong interference between the $b_1(1235)$ bands and the σ amplitude; this interference provides an accurate determination of the phase δ_σ of the σ as a function of $\pi\pi$ mass.

The polarisation of the ω is along the normal to its decay plane. The $f_2(1270)$ components in the data have angular correlations with this normal which are distinctively different from those of the σ ; as a result, f_2 and σ are well separated in the mass range where the σ amplitude is sizable, up to 1000 MeV. Above this mass, the σ amplitude is swamped by the $f_2(1270)$ peak.

The amplitude analysis follows the conventional isobar model. The amplitude for the $b_1(1235)\pi$ final state is parametrised as $\exp(i\Delta_{b_1})F(b_1)$ and that for the ω is parametrised as $\exp(i\Delta_\sigma)F(\sigma \rightarrow \pi\pi)$. Here Δ_{b_1} and Δ_σ are constants describing the strong interaction phases of the 3-body final states $b_1\pi$ and $\omega\sigma$. The $F(b_1)$ amplitude is a Breit-Wigner amplitude of constant width for $b_1(1235)$. A detail is that both S and D-wave decays of $b_1 \rightarrow \omega\pi$ are included, and the D/S ratio of amplitudes is fixed to the PDG value of 0.29 [5].

The $F(\sigma \rightarrow \pi\pi)$ amplitude is taken as [3]:

$$F(\sigma \rightarrow \pi\pi) = \frac{G_\sigma}{M^2 - s - iM\Gamma_{tot}(s)}, \quad (2)$$

$$\Gamma_{tot}(s) = g_1 \frac{\rho_{\pi\pi}(s)}{\rho_{\pi\pi}(M^2)} + g_2 \frac{\rho_{4\pi}(s)}{\rho_{4\pi}(M^2)}, \quad (3)$$

$$g_1 = (b_1 + b_2s) \frac{s - m_\pi^2/2}{M^2 - m_\pi^2/2} \exp[-(s - M^2)/a]. \quad (4)$$

Here $\rho_{\pi\pi}$ is the usual $\pi\pi$ phase space $2k/\sqrt{s}$ and k is the momentum in the $\pi\pi$ rest frame. This formalism includes the Adler zero explicitly into $\Gamma(s)$; the exponential factor cuts off the width at large s . This formula has been fitted simultaneously to BES data [1], CERN-Munich data [4] and the K_{e4} data of Pisluk et al. [5]. Our objective is to determine the phase

$$\delta_\sigma(s) = \tan^{-1} \left(\frac{M\Gamma(s)}{M^2 - s} \right). \quad (5)$$

A small detail is that eqn. (2) should strictly contain a dispersive correction to the real part of the amplitude. However, over the mass range covered here, this correction is very small because the phase rises almost linearly with s . The term $b_1 + b_2s$ fitted to the data accomodates this small correction.

Another technical detail is that there are actually two $J/\Psi \rightarrow \omega\sigma$ amplitudes having orbital angular momenta $L = 0$ and 2 in the production process.

These are both included in the fit, with different coupling constants and different strong interaction phases Δ_σ . A centrifugal barrier for production with $L = 2$ is included, but has little effect since the momentum in the $\omega\sigma$ final state is large. Likewise, $L = 0$ and 2 are both possible for $J/\Psi \rightarrow b_1(1235)\pi$; in practice the $L = 2$ amplitude is small.

In the fitting procedure, all amplitudes except that for $\omega\sigma$ are fitted to the whole data set. In order to determine the phase variation of the σ amplitude with mass, slices 100 MeV wide are examined from $M_{\pi\pi} = 400$ to 1000 MeV. Lower masses are not accessible because the b_1 band runs off the corner of the Dalitz plot; as a reminder, $s_{\pi\pi}$ varies linearly as one moves perpendicular to the σ band, with the result that low masses are compressed tightly towards the edge of the Dalitz plot.

The determination of δ_σ has been done in four ways with progressively increasing freedom in the fit, in order to check for consistency. Results are shown as points with errors in panels (a)–(d) of Fig. 2. In the first (most restrictive) approach (a), only one bin of $\pi\pi$ mass is examined at a time. The σ amplitude is fitted to the whole $\pi\pi$ mass range, but allowing a perturbation to the phase δ_σ of the Breit-Wigner amplitude in a single bin. In the second approach (b), both magnitude and phase of $F(\sigma \rightarrow \pi\pi)$ are set free in one bin at a time. In Fig. 2(c), the phase is set free in all bins simultaneously, but the magnitude is fitted to the whole mass range in accordance with eqns. (2)–(4). In Fig. 2(d), the magnitude and phase are fitted freely in all bins simultaneously. Coupling constants of all other amplitudes are re-optimised for every fit.

The full curve of Fig. 2(a) shows the optimum fit to the whole mass range using eqns. (2)–(4). The strong interaction phase difference $\Delta_{b_1} - \Delta_\sigma$ produces an offset, which is furthermore different for $L = 0$ and $L = 2$ amplitudes; only the phase variation with mass is meaningful. The curve is therefore drawn so that $\delta_\sigma = 0$ at the $\pi\pi$ threshold. It turns out that the phases Δ_{b_1} and Δ_σ are such that the $\omega\sigma$ and $b_1\pi$ amplitudes differ by 90° in phase at a $\pi\pi$ mass of 600 MeV. The interference term between the two amplitudes depends on the cosine of the phase difference, and is therefore determined with maximum sensitivity at this mass.

The dashed curve of Fig. 2(a) shows an alternative fit using for the σ a Breit-Wigner amplitude of constant width. In this case, the offset $\Delta_{b_1} - \Delta_\sigma$ is different because the fitted mass M is different; the curve is therefore adjusted to reproduce the same phase as the full curve at 550 MeV, for purposes of

comparison. The dotted curve shows a fit using a Breit-Wigner amplitude where $\Gamma(s) \propto \rho_{\pi\pi}(s)$; again it is fixed to the same phase as the full curve at 550 MeV, to allow a clear comparison with the other two fits.

There is only small discrimination between the first two forms. The agreement of phases with the curves demonstrates the correlation of magnitude and phase expected from analyticity. The third form, $\Gamma \propto \rho(s)$ (dotted curve), gives a somewhat poorer fit with slightly too large a phase variation. It also suffers from the defect that it gives a virtual state pole below the $\pi\pi$ threshold at $M_{\pi\pi} \sim 232$ MeV [3,6].

We consider the fit of Fig. 2(c) the most realistic. In (b) and (d), there is statistical noise of $\sim \pm 15\%$ in the intensity fitted to individual bins. This noise is obviously unphysical, since the σ amplitude should vary smoothly with mass; noise in the magnitude introduces noise into the phase via correlations in the real part of the interference. Errors on phases are therefore over-estimated in (b) and (d).

It comes as no surprise that δ_σ is accurately determined. In Ref. [1], it was found that all three forms give pole positions in agreement within ± 39 MeV for the real part and within ± 42 MeV for the imaginary part. The extrapolation from the Real s axis to the pole requires that real and imaginary parts of the σ amplitude are separately well determined. This requires that the phase is also well determined as a function of mass.

The determination of δ_σ is insensitive to the precise mass and width of the b_1 . This is because the σ and b_1 bands cross on the Dalitz plot at an angle of 45° and the data integrate over the line-shape of the b_1 .

In fitting $\pi\pi$ elastic data, we adopt the Dalitz-Tuan prescription [7], adding phases of σ and $f_0(980)$ amplitudes. [The $f_0(1370)$ and $f_0(1500)$ contributions are likewise added in, but are very small]. This prescription guarantees that unitarity is satisfied up to the inelastic threshold. The dashed curve of Fig. 3 shows the σ phase δ_σ from eqn. (5); the full curve shows the sum of all contributions. There is satisfactory agreement with K_{e4} data (triangles), CERN-Munich data (black squares) and charge-exchange data (open circles), though there is some discrepancy between the latter two above 700 MeV; the fit goes midway between these two sets of data.

The phase information places restrictions on models of the σ . Although a Breit-Wigner amplitude of constant width fits production data, it gives the absurd result for elastic scattering that $\delta_\sigma = 63^\circ$ at threshold. This requires a compensating background phase of $\sim -63^\circ$ at all masses; this is unphysical,

since left-hand cuts cannot reproduce such a behaviour.

A Breit-Wigner amplitude with $\Gamma \propto \rho(s)$ likewise requires a large background phase in elastic scattering $\sim -50^\circ$ at threshold. A fit to elastic scattering then requires a background phase which drops rapidly from zero at threshold to $\sim -50^\circ$. The Ishida group has shown that elastic data may be fitted with a repulsive background phase linearly proportional to centre of mass momentum and a Breit-Wigner amplitude with $\Gamma \propto \rho(s)$; the scattering length is rather larger than experiment [10]. A more complicated background phase corrects this defect [11] and also remove the virtual-state pole below threshold.

Angular distributions are shown in Fig. 4 for four ranges of $\pi\pi$ mass. The angle χ is the azimuthal angle between the production plane of $J/\Psi \rightarrow \omega X$ and the decay plane $X \rightarrow \pi\pi$. The angle θ_ω is the production angle of the ω in the J/Ψ rest frame. The angle α_π is the decay angle of the π^+ in the rest frame of X , taken with respect to the direction of the recoil ω . The angle β_π is the angle of the π^+ with respect to the direction of X in the rest frame of the ω . The third distribution, $\cos \alpha_\pi$ departs significantly from isotropy. This effect was observed in the earlier DM2 data [12]. Up to $M(\pi\pi) = 700$ MeV, the departure from isotropy is due entirely to interference with $b_1(1235)$; above 800 MeV, interference with $f_2(1270)$ begins to play a role. Up to 800 MeV, there is no evidence for any significant $\pi\pi$ D-wave amplitude. In (d), one sees a strongly varying decay angular distribution due to $f_2(1270)$.

In summary, $\pi\pi$ elastic data and BES production data agree well for the phase variation of the σ amplitude with mass from 450 to 950 MeV. This result is consistent with a single σ resonance with s -dependent width due to the Adler zero; however, some non-resonant background phase could be present in addition.

I wish to thank the Royal Society for funding this work and the BES collaboration for making the data available as part of contracts Q772 between the Royal Society, the Chinese Academy of Sciences and BES.

References

- [1] J.S. Bai et al., *The σ pole in $J/\Psi \rightarrow \omega\pi^+\pi^-$* , hep-ex/0406038 and Phys. Lett. B (to be published).

- [2] Particle Data Group, Phys. Rev. D66 (2002) 010001.
- [3] D.V. Bugg, Phys. Lett. B572 (2003) 1.
- [4] B. Hyams et al., Nucl. Phys. B64 (1973) 134.
- [5] S. Pislak et al., Phys. Rev. Lett. 87 (2001) 221801.
- [6] H.Q. Zheng, hep-ph/0304173.
- [7] R.H. Dalitz and S. Tuan, Ann. Phys. (N.Y.) 10 (1960) 307.
- [8] K. Takamatsu et al., Nucl. Phys. A675 (2000) 312; K. Takamatsu et al., Prog. Theor. Phys. 102 (2001) E52.
- [9] J. Gunter et al., Phys. Rev. D64 (2001) 072003.
- [10] S. Ishida et al., Prog. Theor. Phys. 95 (1996) 745.
- [11] S. Ishida et al., Prog. Theor. Phys. 98 (1997) 1005.
- [12] J.E. Augustin et al., Nucl. Phys. B320 (1989) 1.

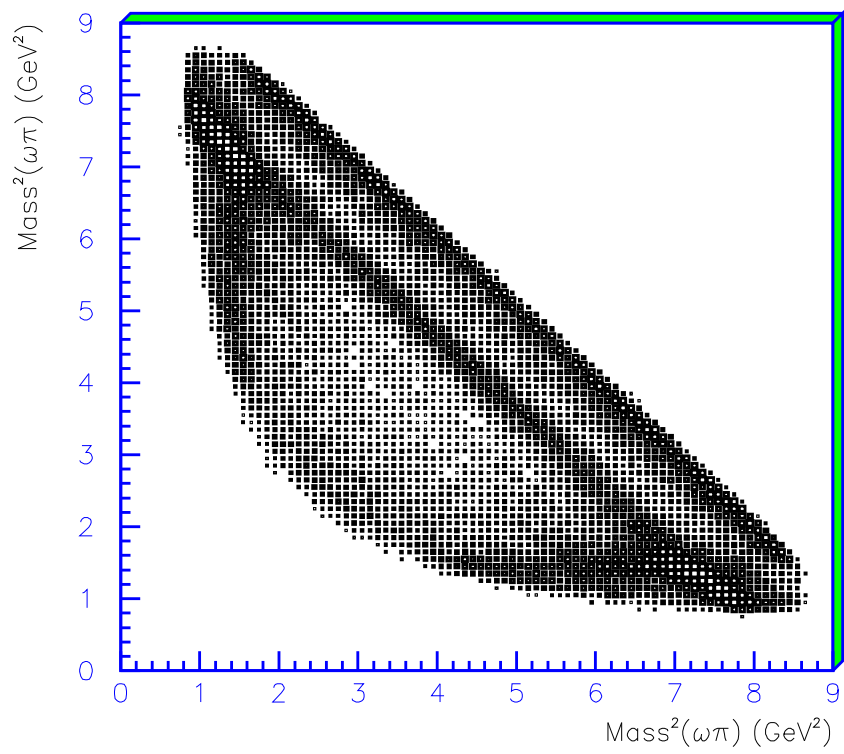


Figure 1: The Dalitz plot for $\omega\pi^+\pi^-$.

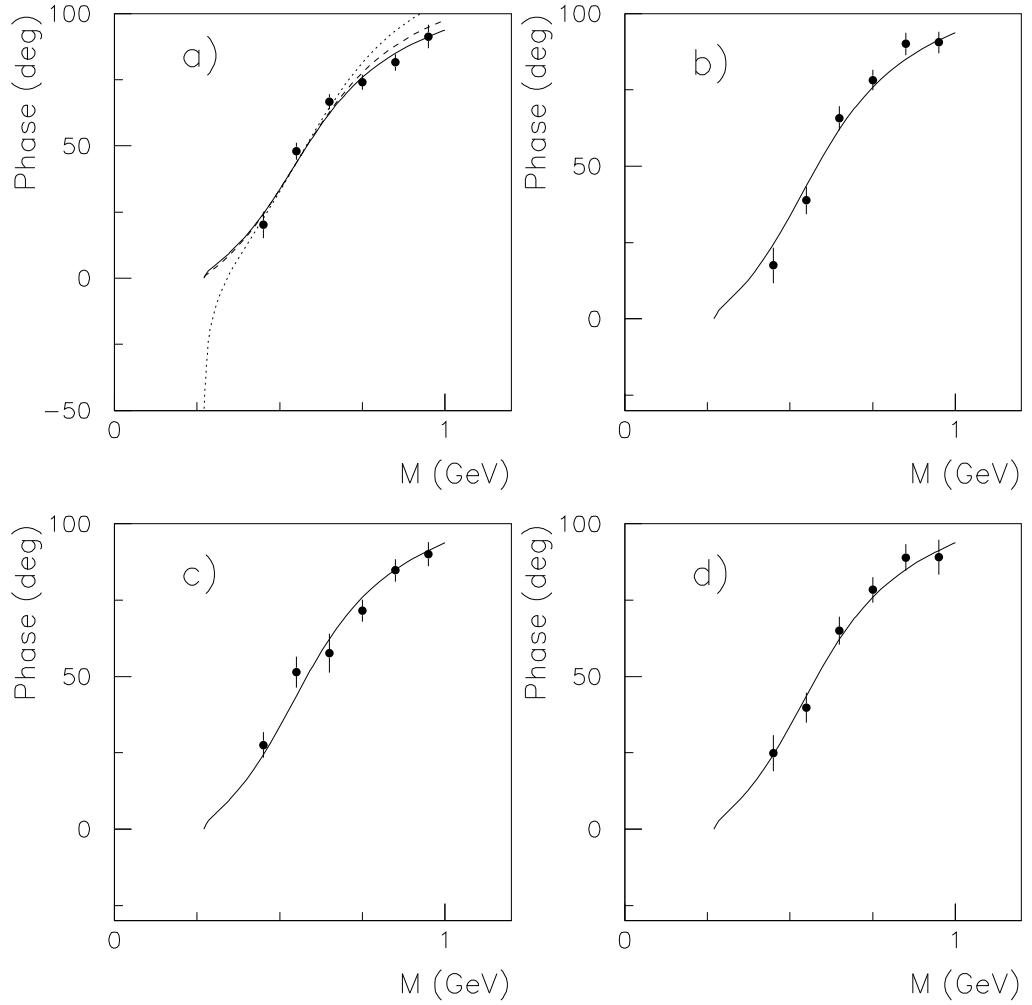


Figure 2: The phase of the $\pi\pi$ S-wave amplitude. The full curve shows the fit from eqns. (2)–(4) to both BES data and elastic scattering data; the dashed curve shows the fit with a Breit-Wigner amplitude of constant width, and the dotted curve the fit with $\Gamma(s) \propto \rho(s)$; points with errors show results fitted to slices of $\pi\pi$ mass 100 MeV wide. In (a), the phase is fitted one bin at a time; in (b) magnitude and phase are fitted one bin at a time; in (c), phases are fitted in all bins simultaneously; in (d) magnitudes and phases are fitted to all bins simultaneously. ⁸

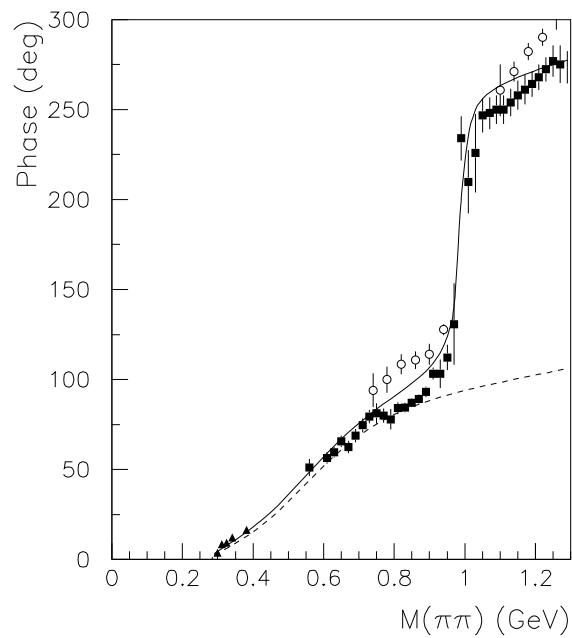


Figure 3: Fit to elastic scattering data. Dashed curve: σ component from eqns. (2)–(4); full curve: full fit; triangles, K_{e4} data [4]; black squares, Cern-Munich data [3]; open circles, charge exchange data [8,9].

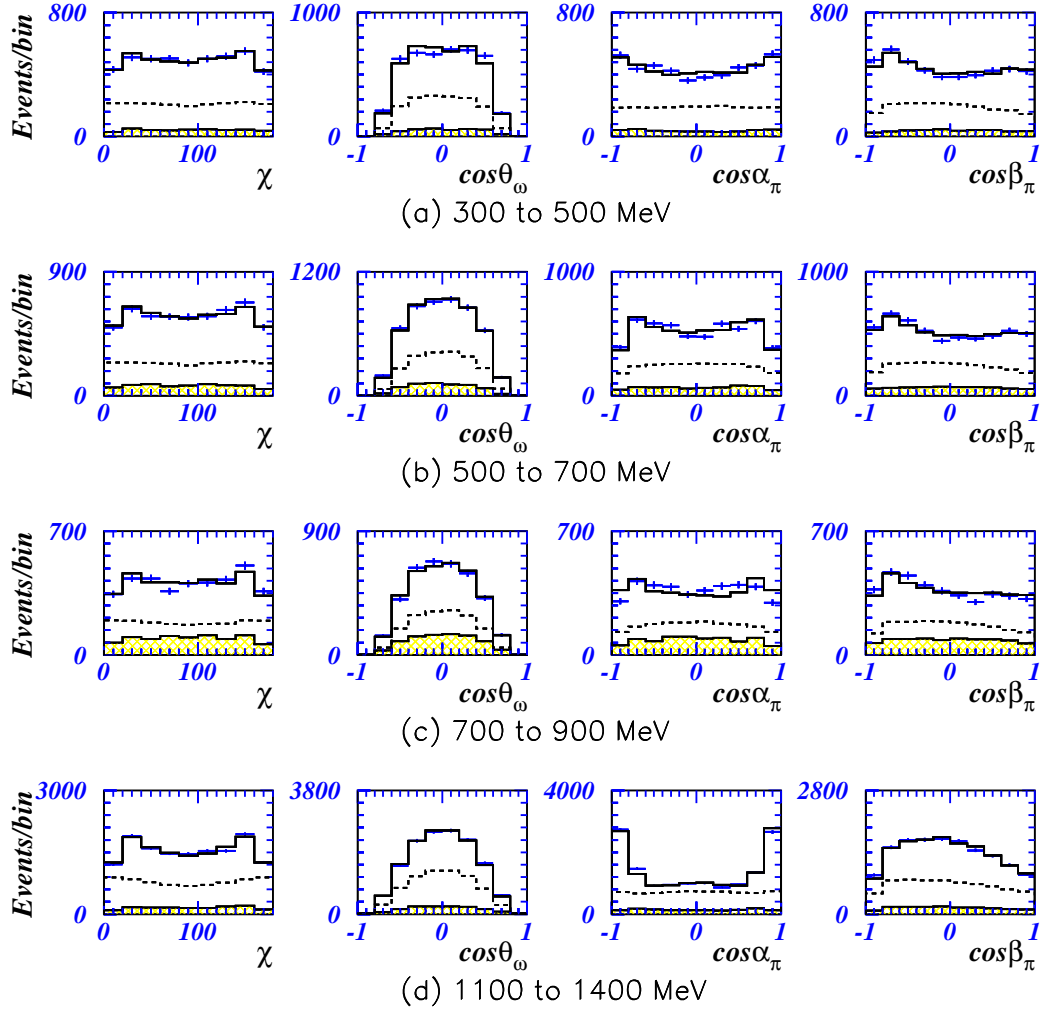


Figure 4: Angular distributions (uncorrected for acceptance) for angles χ , θ_ω , α_π and β_π defined in the text; histograms show the fit for four ranges of $\pi\pi$ mass. The lower histograms in each panel show backgrounds. Dashed curves show the acceptance.